OPEN

NPG Asia Materials (2015) 7, e198; doi:10.1038/am.2015.72

www.nature.com/am

ORIGINAL ARTICLE

Electric-field switching of perpendicularly magnetized multilayers

Yasuhiro Shirahata[1], Ryota Shiina[1], Diego López González[2], Kévin JA Franke[2], Eiji Wada[1], Mitsuru Itoh[1], Nikolay A Pertsev[3], Sebastiaan van Dijken[2] and Tomoyasu Taniyama[1]

Perpendicularly magnetized layers are used widely for high-density information storage in magnetic hard disk drives and nonvolatile magnetic random access memories. Writing and erasing of information in these devices is implemented by magnetization switching in local magnetic fields or via intense pulses of electric current. Improvements in energy efficiency could be obtained when the reorientation of perpendicular magnetization is controlled by an electric field. Here, we report on reversible electric-field-driven out-of-plane to in-plane magnetization switching in Cu/Ni multilayers on ferroelectric $BaTiO_3$ at room temperature. Fully deterministic magnetic switching in this hybrid material system is based on efficient strain transfer from ferroelastic domains in $BaTiO_3$ and the high sensitivity of perpendicular magnetic anisotropy in Cu/Ni to electric-field-induced strain modulations. We also demonstrate that the magnetoelectric coupling effect can be used to realize 180° magnetization reversal if the out-of-plane symmetry of magnetic anisotropy is temporarily broken by a small magnetic field.
NPG Asia Materials (2015) **7,** e198; doi:10.1038/am.2015.72; published online 10 July 2015

INTRODUCTION

Various studies have been published on electric-field-controlled magnetic effects in recent years, including magnetic domain wall propagation,[1–8] magnetic phase transitions,[9–12] spin polarization,[13,14] magnetic anisotropy[15–32] and exchange bias.[33–37] Electric-field control of perpendicular magnetic anisotropy (PMA) would open up new prospects for the realization of high-density magnetic memory and logic technologies operating at low energy consumption levels. Attempts to attain this goal have mostly focused on charge accumulation or band shifting in ultrathin ferromagnetic layers with a metal oxide gate dielectric.[15–20] In these systems, stable reversal of perpendicular magnetization can be realized when precessional motion of magnetization is triggered by short voltage pulses.[19,20] Giant modulations of PMA have also been obtained by voltage control of oxygen ion migration in metal/metal oxide bilayers.[32] Another popular approach towards the engineering of electric-field-controlled magnetic properties is based on interfacial mechanical strain coupling between ferromagnetic and ferroelectric materials in multiferroic hybrids.[4–6,8,10,12,21–31,38] In this case, transfer of lattice strains across interfaces alters the magnetoelastic anisotropy of a ferromagnetic layer via inverse magnetostriction. Anisotropy modulations of more than one order of magnitude have been obtained, which has enabled full electric-field control of the magnetization orientation in two-phase multiferroic systems. However, in spite of intense research efforts in recent years, efficient electric-field control via strain coupling has thus far been limited to ferromagnetic films with in-plane magnetization. Although small modulations of PMA have been shown[21,27–29] and reversal of local magnetic areas has been demonstrated,[30] fully deterministic and reversible electric-field-induced switching between perpendicular and in-plane magnetization states in uniform films has remained elusive despite its technological relevance.

Here, we report on purely electric-field-driven 90° magnetization switching in PMA-Cu/Ni multilayers on $BaTiO_3$ at room temperature. Magnetization rotation in our strain-coupled system is fully reversible and repeatable. Also, we demonstrate that 180° magnetization reversal is obtained in an electric field when the out-of-plane symmetry of PMA is temporarily broken by a small magnetic field. Electric-field-induced magnetic switching is driven by large variations of magnetic anisotropy in the Cu/Ni multilayer originating from ferroelastic domain switching in $BaTiO_3$. The electric field that is required to reorient the magnetization is modest and strict limitations on the total multilayer thickness are not imposed. Our results do therefore present a new and promising realization of fully electric-field-controlled magnetization switching in a PMA system.

MATERIALS AND METHODS

Multilayer growth

$[Cu(9\,nm)/Ni(2\,nm)]_5/Cu(9\,nm)$ multilayers were grown by molecular beam epitaxy on nominally in-plane [100]-poled $BaTiO_3$ single-crystal substrates in an ultrahigh vacuum chamber with a base pressure below 10^{-10} Torr.[39] Before Cu and Ni deposition, a 1-nm thin Fe buffer layer was grown at 300 °C. All Cu and Ni layers were deposited at room temperature and the multilayers were covered by 5 nm of Au to prevent oxidation during sample characterization. The growth process was monitored by reflection high-energy electron

[1]Materials and Structures Laboratory, Tokyo Institute of Technology, Yokohama, Japan; [2]NanoSpin, Department of Applied Physics, Aalto University School of Science, FI-00076 Aalto, Finland and [3]A. F. Ioffe Physical-Technical Institute and Peter the Great St. Petersburg Polytechnic University, St. Petersburg, Russia
Correspondence: Professor T Taniyama, Materials and Structures Laboratory, Tokyo Institute of Technology, 4259 Nagatsuta, Midori-ku, Yokohama 226-8503, Japan.
E-mail: taniyama.t.aa@m.titech.ac.jp
Received 2 December 2014; revised 28 April 2015; accepted 30 April 2015

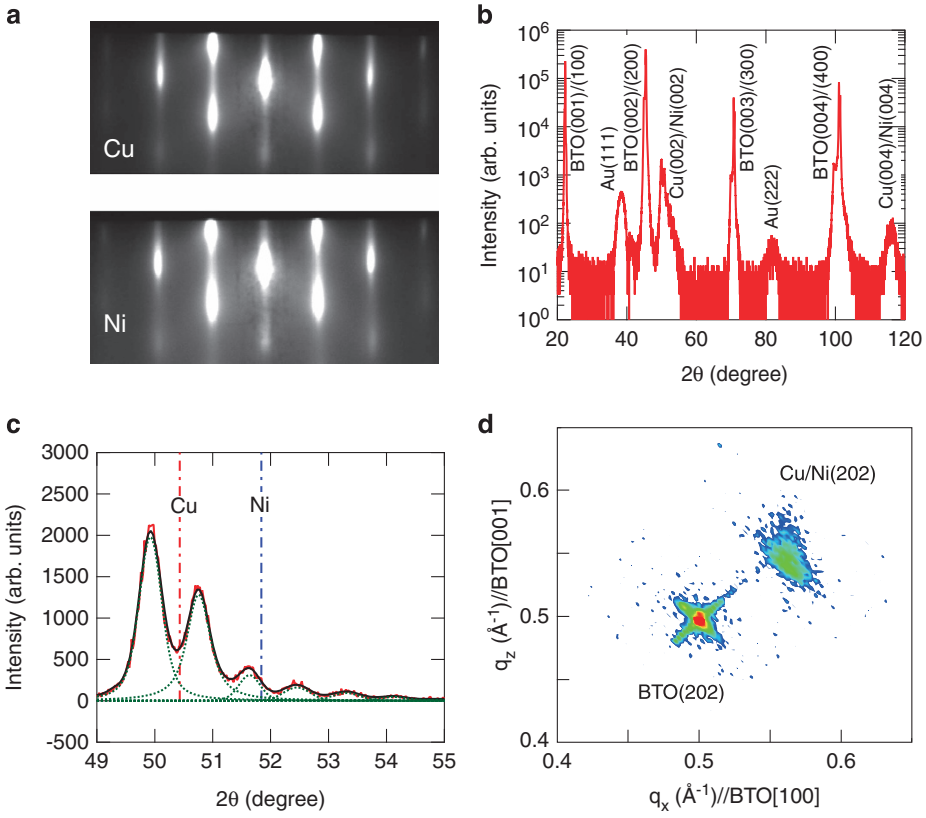

Figure 1 (**a**) RHEED images of the top Ni and Cu layers along the ⟨100⟩ direction of $BaTiO_3$. (**b**) X-ray diffraction spectrum of a $[Cu(9\,nm)/Ni(2\,nm)]_5/Cu(9\,nm)/Fe(1\,nm)/BaTiO_3(001)$ heterostructure and (**c**) an expanded view of an interference fringe from the Cu/Ni multilayer. The black solid curve in **c** is a fit to the experimental data using Voigt functions (green dotted lines) to match the satellite peaks. The red and blue dash-dotted lines indicate the diffraction angles of bulk Cu(002) and Ni(002). (**d**) Reciprocal lattice map around the (202) diffraction peaks of the Cu/Ni multilayer and $BaTiO_3$ substrate.

diffraction (RHEED) and detailed structural analysis was performed using an X-ray diffraction (XRD) measurement system with Cu *K*α radiation.

Magnetic and ferroelectric characterization

Electric-field-induced magnetic switching in the Cu/Ni multilayers was studied using the magneto-optical Kerr effect (MOKE). A laser-based MOKE setup with polar and longitudinal measurement geometries and a laser spot diameter of about 500 μm was used to record magnetic hysteresis curves in an out-of-plane electric field of up to $\pm 10\,kV\,cm^{-1}$. Time-resolved MOKE measurements were conducted using a digital oscilloscope (WavePro 7100A, Teledyne LeCroy, NY, USA) with a sampling rate of $20\,GS\,s^{-1}$ and a bandwidth of 1 GHz. MOKE microscopy was performed to visualize the evolution of the magnetic domain structure in an applied electric field and to measure local magnetic hysteresis curves in polar Kerr geometry. Polarization switching in the $BaTiO_3$ substrate was measured using a ferroelectric materials tester (TF Analyzer 2000, aixACCT Systems, Aachen, Germany) and differential interference contrast microscopy.

RESULTS

Structural characterization

Figure 1a shows reflection high-energy electron diffraction patterns of the top Ni and Cu layers of a $[Cu(9\,nm)/Ni(2\,nm)]_5/Cu(9\,nm)/Fe(1\,nm)/BaTiO_3(001)$ multiferroic heterostructure. The high-energy electron diffraction patterns confirm fully epitaxial film growth with an in-plane orientation of $[100]Ni \parallel [100]Cu \parallel [110]Fe \parallel [100]BaTiO_3$. The X-ray diffraction spectrum of Figure 1b confirms that secondary phases are absent in the Cu/Ni multilayer. The $BaTiO_3$ substrate exhibits a tetragonal crystal structure at room temperature with lattice constants $a_{BTO} = 3.992$ Å and $c_{BTO} = 4.036$ Å and a ferroelectric polarization aligned along the *c* axis. The splitting of the $BaTiO_3$ reflections into (*h*00) and (00*l*) peaks signifies the coexistence of two types of ferroelectric domains. Domains with in-plane ferroelectric polarization (hereafter referred to as *a*-domains) exhibit a rectangular in-plane lattice structure ($x_1 = a_{BTO}$ and $x_2 = c_{BTO}$) and an out-of-plane lattice spacing of $x_3 = a_{BTO}$. The *a*-domains are separated by domains with a perpendicular-to-plane polarization (*c*-domains). The in-plane lattice structure of the *c*-domains is square ($x_1 = x_2 = a_{BTO}$) and $x_3 = c_{BTO}$. Since the $BaTiO_3$ (*h*00) reflections are more intense than the corresponding (00*l*) peaks, the *a*-domains are larger than the *c*-domains in the pristine $BaTiO_3$ substrate. From the integrated intensities of the split peaks, the total sample coverage of *a*-domains is estimated as 93% in this sample.

Figure 1c shows a clear X-ray diffraction interference fringe from the Cu/Ni multilayer. The pronounced satellite peaks are a signature of high structural quality and smooth interfaces. The Cu/Ni bilayer thickness *D* can be calculated from the angular positions of the satellite peaks, which are decomposed into Voigt functions[40]

$$D = \frac{n\lambda}{2|\sin\theta_n - \sin\theta_0|}. \quad (1)$$

Here, θ_n and θ_0 are the diffraction angles of the *n*th order satellite and the fundamental Bragg peak, and λ is the X-ray wavelength. Fitting of the experimental data using Equation 1 gives $D = 11.6$ nm, which is compatible with the nominal layer thickness of the Cu(9 nm)/Ni (2 nm) bilayer.

The shift of the Cu(002)/Ni(002) reflection from the diffraction angles of bulk Cu(002) ($a_{Cu} = 3.615$ Å) and bulk Ni(002) ($a_{Ni} = 3.524$ Å)

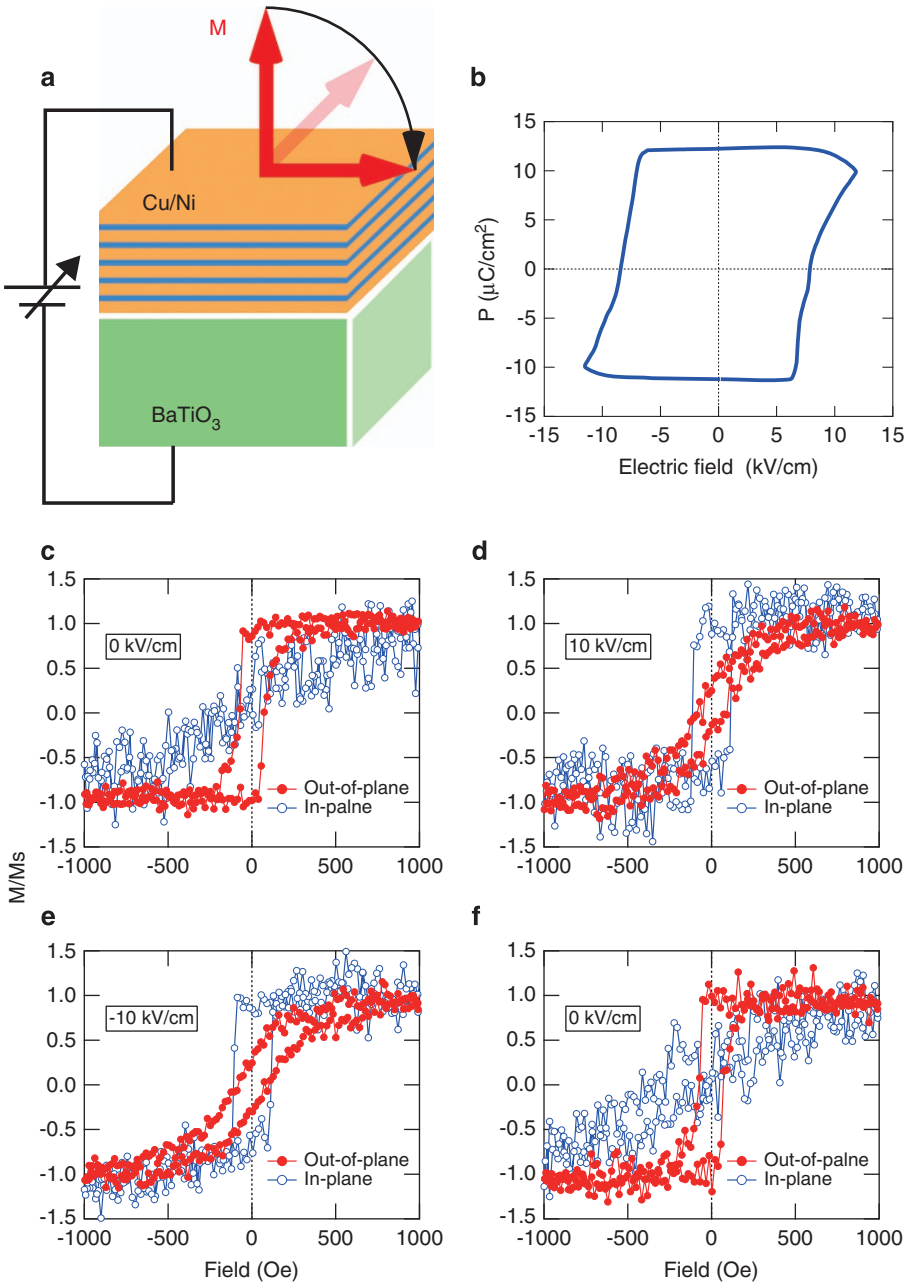

Figure 2 (**a**) Schematic illustration of the experimental system. (**b**) Out-of-plane polarization hysteresis curve of the $BaTiO_3$ substrate. (**c**–**f**) Normalized out-of-plane and in-plane magnetic hysteresis curves of the Cu/Ni multilayer recorded while sequentially applying an electric field of (**c**) $E=0\,kV\,cm^{-1}$, (**d**) $E=10\,kV\,cm^{-1}$, (**e**) $E=-10\,kV\,cm^{-1}$ and (**f**) $E=0\,kV\,cm^{-1}$ across $BaTiO_3$.

reveals a mean out-of-plane lattice spacing of 3.673 Å. Reciprocal lattice maps around the (002) and (202) diffraction peaks indicate a corresponding in-plane lattice spacing of 3.590 Å for the as-grown Cu/Ni multilayer on $BaTiO_3$. The lattice strain in the Ni layers is thus tensile and amounts to 1.9%. This experimental value is in excellent agreement with a theoretical calculation based on the actual thicknesses of Cu (9 nm) and Ni (2 nm) and their elastic stiffness, which yields an in-plane lattice constant of 3.592 Å for a coherent free-standing Cu/Ni multilayer. We note that the reciprocal lattice map around the (202) diffraction peak shown in Figure 1d clearly shows that the misfit strain caused by the lattice mismatch between the Ni/Cu multilayer and $BaTiO_3$ substrate is relaxed in the epitaxially grown film. A detailed theoretical analysis of strain and magnetic anisotropy is given after the next section.

Electric-field-driven 90° magnetization switching

Cu/Ni multilayers were selected for this study because they provide strong PMA in a relatively large Ni thickness range (typically $1.5\,nm < t_f < 8\,nm$).[41] Moreover, since PMA in Cu/Ni originates from a magnetoelastic effect, it is predicted to be sensitive to electric-field-induced strain modulations.[38] Figure 2 shows the experimental configuration, polarization switching in $BaTiO_3$, and normalized out-of-plane and in-plane magnetic hysteresis curves for different electric fields across the $BaTiO_3$ substrate. The data in Figures 2c–f provide macroscopic information about the magnetic configuration at room temperature and were recorded using a MOKE setup with polar and longitudinal measurement geometries. Before applying any electric field (Figure 2c), a square-shaped out-of-plane hysteresis curve

is obtained while the in-plane one is slanted and almost completely unopened. These measurements clearly establish that the Cu/Ni multilayer exhibits PMA in the as-grown state. The slope of the in-plane magnetic hysteresis curve corresponds to a magnetic anisotropy strength of $K_{\mathrm{eff}} \approx 2.4 \times 10^4\,\mathrm{J\,m^{-3}}$. When a positive electric field of $10\,\mathrm{kV\,cm^{-1}}$ is applied to $BaTiO_3$ (Figure 2d), the shapes of both hysteresis curves change instantaneously. Now the out-of-plane curve is slanted and the in-plane hysteresis curve is square. This apparent reversal in the shape of the hysteresis curves indicates a rotation of the easy magnetization axis from perpendicular ($E = 0\,\mathrm{kV\,cm^{-1}}$) to in-plane ($E = 10\,\mathrm{kV\,cm^{-1}}$), as illustrated in Figure 2a. A very similar result is obtained for a negative electric field of $-10\,\mathrm{kV\,cm^{-1}}$ (Figure 2e). The electric-field-induced magnetic switching effect does therefore not depend on the polarity of the applied bias voltage. Finally, when the electric field is switched off (Figure 2f), the magnetization of the Cu/Ni multilayer rotates back to a perpendicular direction. We note that the electric-field-controlled switching sequence of Figure 2 is fully repeatable over many on/off cycles of applied bias voltage. Moreover, the magnitude of the electric-field-driven effect is very large. The converse magnetoelectric coupling coefficient $\alpha = \mu_0 \Delta M_S / E$ amounts to $6 \times 10^{-7}\,\mathrm{s\,m^{-1}}$, which is the highest reported magnetoelectric coupling efficiency for a strain-coupled PMA system. Modest electric-field strengths of $\pm 10\,\mathrm{kV\,cm^{-1}}$ were used in the switching experiments because it suffices to saturate the polarization of the $BaTiO_3$ substrate in a perpendicular-to-plane direction (Figure 2b and Figure 3).

Information about the magnetic microstructure of the Cu/Ni multilayer is provided by MOKE microscopy. The images presented in Figure 3a show the evolution of the magnetic domain structure as a function of out-of-plane electric field. In the initial remanent state (①), the sample consists of elongated magnetic stripe domains with alternating perpendicular and mostly in-plane magnetizations. The application of a small electric field of $2\,\mathrm{kV\,cm^{-1}}$ switches the magnetization into the film plane via fast lateral growth of in-plane magnetized domains (②–③). The magnetic configuration of ③ does not change upon further increase of the electric-field strength. When the electric field is switched off, perpendicularly magnetized stripe domains are restored (④). Reversal of the out-of-plane electric-field direction first enlarges the perpendicular magnetic domains (⑤–⑥), but the process is suddenly reversed at an electric field of $-2.5\,\mathrm{kV\,cm^{-1}}$ (⑦). A further increase of the electric field promotes the growth of domains with in-plane magnetization (⑧) until saturation is reached at $E = -4\,\mathrm{kV\,cm^{-1}}$ (⑨). Finally, a magnetic configuration with alternating perpendicular and in-plane domains is again re-established in the Cu/Ni multilayer after the electric field is switched off (⑩). The MOKE microscopy data of Figure 3a indicate that rotation of the easy magnetization axis into the film plane is symmetric in large applied electric fields (③ and ⑨), in agreement with the measurements of Figure 2. However, for small electric fields (that is, below saturation) the response can be asymmetric, depending on the direction of the applied electric field relative to the ferroelectric polarization in the $BaTiO_3$ substrate. Another observation relates to the orientation of magnetization inside the in-plane domains. Although the unopened and slanted hysteresis curves in ③ and ⑨ indicate fully in-plane magnetization in saturation, the hysteresis loops of the same domains are not completely closed in the multidomain

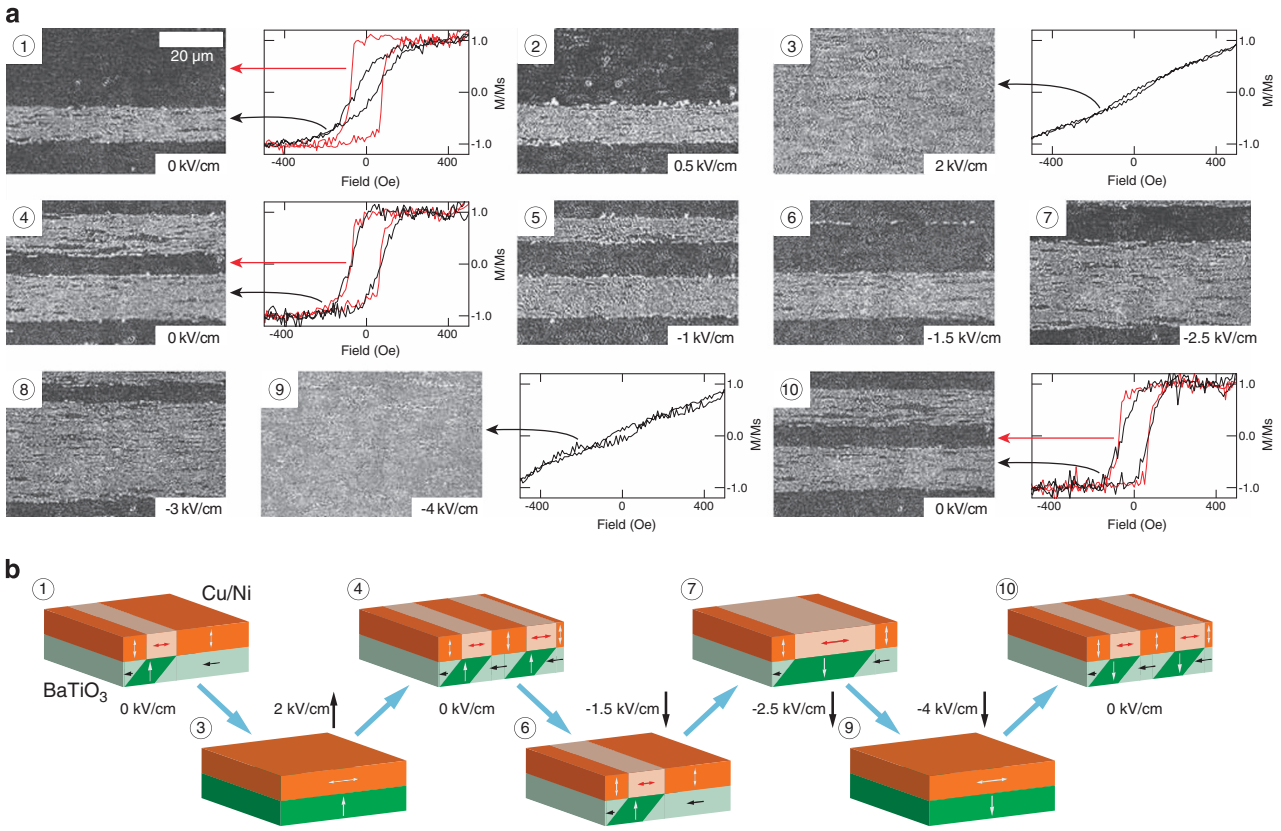

Figure 3 (**a**) MOKE microscopy images (measured in zero magnetic field) and local polar MOKE curves of the Cu/Ni multilayer as a function of out-of-plane electric field. (**b**) Schematic illustration of the ferroelectric domain structure in the $BaTiO_3$ substrate (green) and the magnetic domains of the Cu/Ni multilayer (orange) during the electric-field-controlled switching sequence in **a**.

state. Magnetic contrast within the domains suggest that the magnetization directions are partly perpendicular, which could be caused by coupling to the perpendicular magnetization of neighboring stripe domains.

The electric-field-controlled switching events and magnetic anisotropy modulations are fully explained by considering the ferroelastic domain pattern of the ferroelectric $BaTiO_3$ substrate and interfacial strain transfer to the Cu/Ni multilayer. Molecular beam epitaxy of the Cu/Ni multilayer onto $BaTiO_3$ produces a fully (001)-oriented layered structure with smooth interfaces. However, owing to the significant differences ($>10\%$) between the lattice constants of $BaTiO_3$ and those of Cu and Ni, most of the lattice mismatch strain relaxes at the onset of Cu growth. Hereafter, the Cu/Ni multilayer grows with an in-plane lattice constant of 3.590 Å, which corresponds closely to that of a coherent free-standing Cu/Ni multilayer. Thus, a 1.9% tensile strain is induced in the Ni layers, which is determined by the lattice mismatch between Cu and Ni and the elastic stiffnesses and thicknesses of Cu and Ni layers. From this we conclude that the layers are almost completely decoupled from the ferroelastic $BaTiO_3$ domains in the as-grown state. Since the magnetoelastic coefficient of Ni is positive, the tensile strain induces PMA in the Cu/Ni multilayer.

If an out-of-plane electric field is applied along the direction of ferroelectric polarization in the *c*-domains, these domains grow at the expense of *a*-domains. This ferroelectric switching effect coincides with an abrupt change of the in-plane lattice structure in $BaTiO_3$. In all areas where *a*-domains are replaced by *c*-domains, the lattice constant is reduced by 1.1% along one of the crystallographic axes. Since the Cu/Ni multilayer is firmly clamped to the $BaTiO_3$ substrate, a large fraction of this uniaxial compressive strain is transferred to the Cu and Ni layers. This electric-field-controlled strain effect opposes the original growth-induced tensile strain state, leading to magnetization reorientation from a perpendicular-to-plane to an in-plane direction. Figure 3b illustrates the experimental switching sequence of Figure 3a starting with *c*-domain expansion (①). When the ferroelectric substrate is transformed into a single-domain *c* state, the easy magnetization direction is oriented in the film plane (③). The $BaTiO_3$ substrate relaxes back to a polydomain state with *a*–*c* stripe domains after the electric field is turned off (④). In this case, reversible strain transfer to the Cu/Ni multilayer induces PMA on top of the ferroelectric *a*-domains. When a small electric field is applied against the ferroelectric polarization of the *c*-domains, the *a*-domains grow (⑥) until the perpendicular polarization in the *c*-domains abruptly aligns with the external electric field by 180° switching. Afterwards, the *c*-domains grow at the expense of *a*-domains (⑦) until the single-domain state is reached (⑨). After the electric field is switched off, relaxation into a structure with *a*–*c* domains commences again (⑩). Throughout this sequence of electric fields, the evolution of the ferroelectric domain structure is mimicked by the domains in the Cu/Ni multilayer because of efficient strain transfer and inverse magnetostriction. We note that the electric field that is required to rotate the magnetization in the MOKE microscopy experiments (Figure 3a) is relatively small compared with the switching field in the polarization hysteresis curve of the $BaTiO_3$ substrate (Figure 2b). This difference could be explained by the time-scale of the two measurements or a sample-to-sample variation. Although the polarization hysteresis curve was obtained at 0.2 Hz, the MOKE microscopy data were typically recorded some 10 s after the electric field was set. We would also like to point out that the initial state in Figure 3a, (①) was obtained after the application of an electric field and prolonged domain relaxation. Hence, it does not represent the as-grown state. Directly after growth, no domain correlations between the ferroelectric $BaTiO_3$ substrate and the Cu/Ni multilayer exist because of strong relaxation of lattice mismatch strain in the first Cu layer. As a result, as-grown samples exhibit uniform PMA irrespective of the underlying ferroelectric domain pattern.

Theoretical analysis of strain and magnetic anisotropy

To confirm that interfacial strain transfer from ferroelastic domains in $BaTiO_3$ to the Cu/Ni multilayer explains the experimental results, we analyze the magnetization-dependent part of the free energy of a strained Ni layer written as a function of the direction cosines m_i ($i=1, 2, 3$) of the unit vector $\mathbf{m}=\mathbf{M}/M_s$. In our formulation, the interfacial magnetic anisotropy is incorporated into the volumetric energy density $\Delta F(m_i)$ via the term $K_s m_3^2/t_f$, where t_f is the Ni layer thickness and K_s is the parameter characterizing the sum of specific energies of two Ni/Cu interfaces. In the crystallographic reference frame with the x_3 axis orthogonal to the interfaces, the resulting energy density $\Delta F(m_i)$ can be written as[42]

$$\Delta F \cong K_{1\|} m_1^2 m_2^2 + K_{1\perp}\left(m_1^2+m_2^2\right)m_3^2 + \tfrac{K_s}{t_f}\, m_3^2 + B_1\left(u_1 m_1^2 + u_2 m_2^2\right) - B_1\left[\tfrac{B_1}{6c_{11}} + \tfrac{c_{12}}{c_{11}}(u_1+u_2)\right]m_3^2 + \tfrac{1}{2}\mu_0 M_s^2\left(N_{11}m_1^2 + N_{22}m_2^2 + N_{33}m_3^2\right), \quad (2)$$

where $K_{1\|}(t_f)$ and $K_{1\perp}(t_f)$ are the in-plane and out-of-plane magnetocrystalline anisotropy constants of fourth order,[43] μ_0 is the permeability of vacuum, N_{ii} are the diagonal components of the tensor of demagnetizing factors, u_1 and u_2 are the in-plane normal strains (shear strains are absent in our case), B_1 is the magnetoelastic coefficient[44] and c_{11} and c_{12} are the elastic stiffnesses at fixed **M** (we use the Voigt matrix notation for strains and elastic constants). Using the relations $m_1=\cos\phi\,\sin\theta$, $m_2=\sin\phi\,\sin\theta$ and $m_3=\cos\theta$, we express the energy density ΔF through the polar angle θ and the azimuth angle ϕ of the magnetization direction. Numerical minimization of the function $\Delta F(\phi,\theta)$ allows us to determine the equilibrium magnetization orientations in the cubic Ni layers for different in-plane lattice strains u_1 and u_2. We performed this minimization for Ni films with $t_f=2$ nm and large in-plane dimensions ensuring $N_{11}=N_{22}=0$ and $N_{33}=1$ using the following values of the involved material parameters: $M_s=4.85\times10^5\ \mathrm{A\,m^{-1}}$,[44] $K_s=4.3\times10^{-4}\ \mathrm{J\,m^{-2}}$,[45] $K_{1\|}=-2.5\ 10^4\ \mathrm{J\,m^{-3}}$, $K_{1\perp}=-1.2\times10^4\ \mathrm{J\,m^{-3}}$,[43] $B_1=9.2\times10^6\ \mathrm{J\,m^{-3}}$,[46] $c_{11}=2.465\times10^{11}\ \mathrm{J\,m^{-2}}$ and $c_{12}=1.473\times10^{11}\ \mathrm{J\,m^{-2}}$.[47] In the free-standing multilayer, the lattice matching between the 2-nm thick Ni layers and the 9-nm thick Cu films produces tensile strains $u_1=u_2\cong1.9\%$ in Ni. (This theoretical value is smaller than the nominal misfit strain of 2.58% because Cu layers are slightly compressively strained by Ni ones in elastic equilibrium.) Since the magnetoelastic coefficient B_1 is positive, these strains stabilize a perpendicular magnetization orientation in the Ni layers ($\theta=0$ or 180°). The mechanical interaction between the Ni/Cu multilayer and a thick $BaTiO_3$ substrate creates additional strains δu_1 and δu_2 in the Ni layers. Owing to significant differences between the lattice constants of $BaTiO_3$ and those of Cu, the nominal values δu_i^0 of these tensile strains appear to be very big ($\delta u_1^0\approx12\%$ and $\delta u_2^0\approx 11\%$). The actual substrate-induced strains, however, are much smaller because of effective strain relaxation during the Cu/Ni multilayer growth. This effect may be described by the relations $\delta u_1=\eta\delta u_1^0$ and $\delta u_2=\eta\delta u_2^0$ with $\eta\ll1$. Since the strains δu_1 and δu_2 are tensile, the magnetization of the Ni/Cu multilayer grown on $BaTiO_3$ initially should have a perpendicular orientation irrespective of the parameter η. For $\eta=0$, the model gives $a_{Ni}\cong3.592$ Å and $K_{eff}\approx2.5\times10^4\ \mathrm{J\,m^{-3}}$, which are in excellent agreement with the experimental data ($a_{Ni}=3.590$ Å and $K_{eff}=2.4\times10^4\ \mathrm{J\,m^{-3}}$).

After electric-field-induced switching from an *a*-domain to a *c*-domain, the strain δu_1 becomes $\delta u_1 = \eta \delta u_1^0 + \xi(\delta u_2^0 - \delta u_1^0)$. Here, the strain transfer parameter ξ is expected to be much larger than η because of strong interfacial mechanical coupling between the Cu/Ni multilayer and the $BaTiO_3$ substrate during ferroelectric domain switching. Taking $\eta = 0$ in first approximation, we calculated the equilibrium magnetization orientation after 90° polarization switching in $BaTiO_3$ as a function of the transfer parameter ξ. Figure 4 shows that, at $\xi < 0.073$, the magnetization retains its initial perpendicular direction, whereas at $\xi > 0.193$ it acquires an in-plane orientation ($\theta = 90°$). In the intermediate range of $0.073 \leqslant \xi \leqslant 0.193$ the Ni layers should have a canted magnetization with the polar angle θ gradually increasing with ξ from 0° to 90°. However, due to efficient transfer of piezoelectric strains, ξ is expected to be close to unity in our experimental system.[4] For this scenario the model predicts the formation of two types of magnetic areas in an out-of-plane electric field; one with in-plane magnetization (where the ferroelectric domains underneath have switched from *a*- to *c*-type) and another with perpendicular magnetization (where the ferroelectric domains underneath remain the same as during Cu/Ni multilayer growth). This qualitatively agrees with the MOKE microscopy observations in Figure 3. The theoretical model thus fully supports the experimental observations. We note that other magnetoelectric coupling effects, such as electrostatic charge modulation near the $BaTiO_3$ interface, can be excluded as an explanation for electric-field-controlled switching in the Cu/Ni multilayer. First, the symmetric magnetic response in

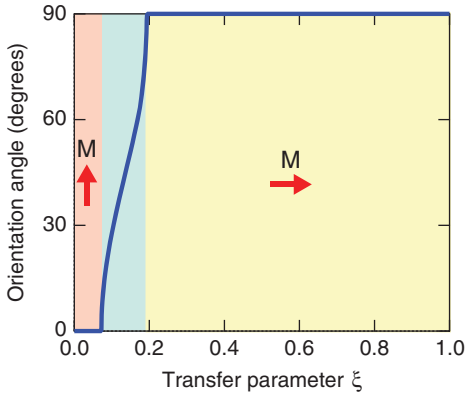

Figure 4 Calculated orientation of the equilibrium magnetization direction in the Cu/Ni multilayer after *a*- to *c*-domain switching in $BaTiO_3$. The parameter ξ indicates the efficiency of strain transfer from the $BaTiO_3$ substrate to 2-nm thick Ni layers during polarization switching.

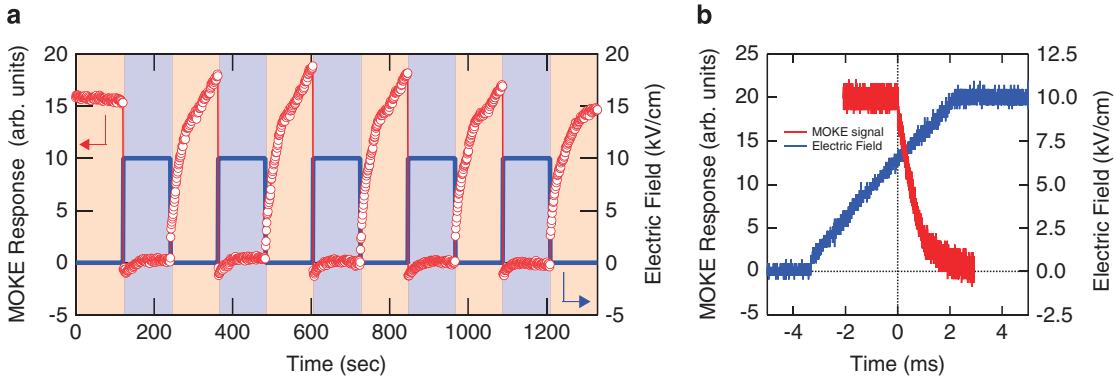

Figure 5 (**a**) Time-resolved polar MOKE response of the Cu/Ni multilayer on $BaTiO_3$ during on and off switching of a 10 kV cm^{-1} electric field. (**b**) Zoom-in of the MOKE response during the application of a positive electric-field pulse.

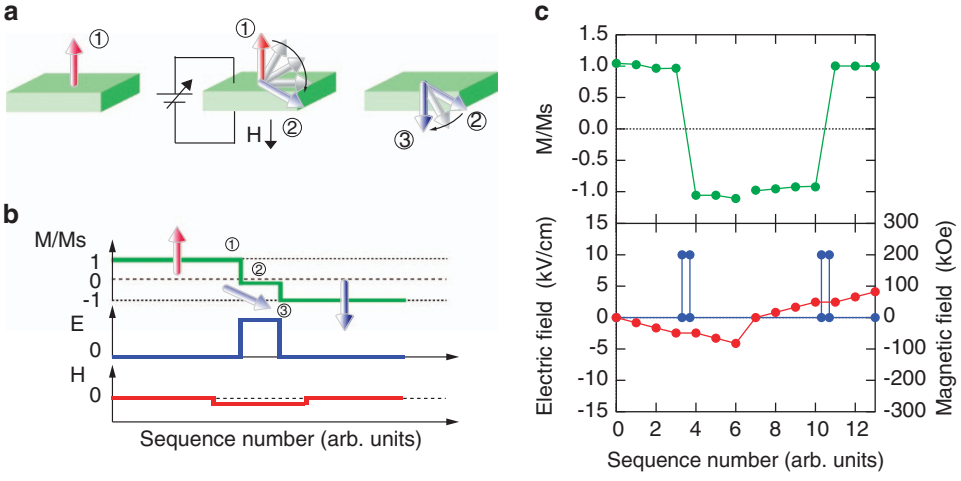

Figure 6 (**a**) Schematic illustrations of the 180° magnetization reversal process. (**b**) Deterministic reversal is obtained by short electric field pulses when a small out-of-plane magnetic field opposes the initial magnetization direction. (**c**) Experimental demonstration of 180° magnetization reversal with an electric field of 10 kV cm^{-1} and a magnetic field of ±50 Oe.

positive and negative electric fields opposes the polarity dependence of charge accumulation. Second, the first Ni layer and the $BaTiO_3$ substrate are separated by a 9-nm thick Cu spacer layer, which exceeds the Thomas–Fermi screening length by more than one order of magnitude.

Time-resolved measurements

The dynamics of electric-field-induced magnetic switching was studied by recording the time-resolved MOKE response of strain-coupled Cu/Ni multilayers during the application of a series of voltage pulses across the $BaTiO_3$ substrate. Figure 5a shows the result for five on/off cycles with an electric field of $10\,kV\,cm^{-1}$. Initially, the sample consists of alternating domains with perpendicular and partly in-plane magnetizations (similar to ④ and ⑩ in Figure 3a). In this state, the polar MOKE signal is large. When an out-of-plane electric field is applied, the MOKE response rapidly drops to zero, indicating fast and complete reorientation of the magnetization into the film plane. After the electric field is turned off, the initial magnetization state is re-established. Back and forth switching between the two magnetization states is thus reversible and repeatable. The results of Figure 5a are again explained by ferroelastic domain transformations in $BaTiO_3$. Importantly, they indicate that the time-scale of strain-driven magnetization reorientation is determined by the rate of electric-field induced $a \rightarrow c$ domain switching in $BaTiO_3$, but not by magnetization dynamics itself. Indeed, as can be seen from Figure 5b, the change in polar MOKE signal commences when the electric field reaches $\sim 7\,kV\,cm^{-1}$, which closely corresponds to the onset of polarization reversal in $BaTiO_3$ (Figure 2b). Beyond this, the magnetization rapidly reorients into the film plane within ~ 2 ms. Since the rise time of the electric-field pulse is ~ 5 ms, the magnetization switching time in this experiment might be limited by the shape of the voltage pulse. Therefore, it should be considered as an upper bound for electric-field-induced magnetic switching in Cu/Ni multilayers. Magnetization reorientation in the off-state (Figure 5a) is not driven by an electric field but rather by ferroelastic domain relaxation in the $BaTiO_3$ substrate, which proceeds more slowly. The small differences in polar MOKE signal after 120 s in the off-state are attributed to minor differences in the ferroelectric *a*–*c* domain patterns during subsequent relaxation processes.

Electric-field-controlled 180° magnetization reversal

Full 180° reversal between two perpendicular magnetization states can be induced by an electric field if the symmetry of PMA in the Cu/Ni multilayers is broken by a small out-of-plane magnetic field. As previously discussed, the application of an electric field to the $BaTiO_3$ substrate reorients the magnetization into the film plane (90° switching effect). Without an external magnetic field, the magnetization switches back to its original perpendicular position after the electric field is turned off (see Figure 5). However, if a small magnetic field is applied in the opposite out-of-plane direction during the electric-field-controlled magnetic switching sequence, full magnetization reversal by 180° is realized. In this instance, the magnetization first rotates by $> 90°$ to a slightly tilted position when the electric field is turned on, and it continues to rotate in the same direction after the electric field is turned off. Figures 6a and b schematically illustrate the 180° switching sequence. The experimental MOKE data of Figure 6c demonstrate that full magnetization reversal in Cu/Ni multilayers on $BaTiO_3$ is indeed obtained. Initially, the magnetization of the multilayer points into one of the perpendicular-to-plane directions ($M/M_S = 1$). The application of a small negative magnetic field of -50 Oe and an electric-field pulse of $10\,kV\,cm^{-1}$ fully reverses the magnetization ($M/M_S = -1$). In Figure 6c, we should note that a decrease in the magnetic field down to -50 Oe does not change the magnetization orientation ($M/M_S = 1$), whereas the electric-field pulse suddenly reverses the magnetization to $M/M_S = -1$ at the constant negative magnetic field of -50 Oe. After the electric-field-induced magnetization reversal, a further decrease in magnetic field beyond the magnetic coercive field of ~ 100 Oe does not change the magnetization values any more. The results clearly corroborate that the magnetization is fully reversed purely by the electric-field pulse. Back-switching is realized when an opposite magnetic field and the same electric-field pulse are applied ($M/M_S = 1$). The 180° magnetic switching effect is thus reversible and it only occurs when a small magnetic field is applied against the original perpendicular-to-plane magnetization direction. Similar to 90° magnetization reorientation, the polarity of the electric field does not affect the 180° switching effect.

CONCLUSIONS

In summary, we have demonstrated reversible electric-field control of magnetic switching in epitaxial Cu/Ni multilayers with PMA on $BaTiO_3$ substrates. Magnetization reversal in this multiferroic heterostructure is driven by efficient interfacial mechanical strain coupling between the Cu and Ni layers and the ferroelastic domains of $BaTiO_3$. Only modest electric fields are required to reorient the magnetization. In addition, the coupling mechanism provides full electric-field control of relatively thick magnetic films. The total multilayer thickness in the reported experiments amounts to 65 nm. Electric-field manipulation of multilayers with similar thicknesses would not be possible by other magnetoelectric coupling effects. The demonstrated ability to deterministically switch relatively thick magnetic films with PMA in small electric fields is potentially interesting for magnetic memories and other devices that could functionally utilize electric-field-controlled manipulation of PMA (for example, in microwave electronics or magnonics). Another property of Cu/Ni multilayers, namely giant magnetoresistance,[48] might also prove useful in this respect, because it renders possible nondestructive readout of local magnetization states.

CONFLICT OF INTEREST

The authors declare no conflict of interest.

ACKNOWLEDGEMENTS

This work was supported in part by Industrial Technology Research Grant Program in 2009 from NEDO, Toray Science Foundation, JSPS KAKENHI (Grant Nos. 24·7390, 25·03065), the Advanced Materials Development and Integration of Novel Structured Metallic and Inorganic Materials Project of MEXT, the European Research Council (ERC-2012-StG 307502-E-CONTROL) and the Collaborative Research Project of the Materials and Structures Laboratory, Tokyo Institute of Technology. YS thanks JSPS Fellowships for Young Scientists and KJAF acknowledges financial support from the Finnish Doctoral Program in Computational Sciences. The work at the Ioffe Physical-Technical Institute was supported by the Government of the Russian Federation through the Program P220 (Project No.14.B25.31.0025).

1 Bauer, U., Emori, S. & Beach, G. S. D. Electric field control of domain wall propagation in Pt/Co/GdOx films. *Appl. Phys. Lett.* **100**, 192408 (2012).
2 Schellekens, A. J., van den Brink, A., Franken, J. H., Swagten, H. J. M. & Koopmans, B. Electric-field control of domain wall motion in perpendicularly magnetized materials. *Nat. Commun.* **3**, 847 (2012).
3 Chiba, D., Kawaguchi, M., Fukami, S., Ishiwata, N., Shimamura, K. & Ono, T. Electric-field control of magnetic domain-wall velocity in ultrathin cobalt with perpendicular magnetization. *Nat. Commun.* **3**, 888 (2012).
4 Lahtinen, T. H. E., Franke, K. J. A. & van Dijken, S. Electric-field control of magnetic domain wall motion and local magnetization reversal. *Sci. Rep.* **2**, 258 (2012).

5 De Ranieri, E., Roy, P. E., Fang, D., Vehsthedt, E. K., Irvine, A. C., Heiss, D., Casiraghi, A., Campion, R. P., Gallagher, B. L., Jungwirth, T. & Wunderlich, J. Piezoelectric control of the mobility of a domain wall driven by adiabatic and non-adiabatic torques. *Nat. Mater.* **12**, 808–814 (2012).
6 Lei, N., Devolder, T., Agnus, G., Aubert, P., Daniel, L., Kim, J.-V., Weisheng, Z., Trypiniotis, T., Cowburn, R. P., Chappert, C., Ravelosona, D. & Lecoeur, P. Strain-controlled magnetic domain wall propagation in hybrid piezoelectric/ferromagnetic structures. *Nat. Commun.* **4**, 1378 (2013).
7 Bauer, U., Emori, S. & Beach, G. S. D. Voltage-controlled domain wall traps in ferromagnetic nanowires. *Nat. Nanotechnol.* **8**, 441–416 (2013).
8 Franke, K. J. A., Van de Wiele, B., Shirahata, Y., Hamalainen, S. J., Taniyama, T. & van Dijken, S. Reversible electric-field-driven magnetic domain wall motion. *Phys. Rev. X* **5**, 011010 (2015).
9 Ohno, H., Chiba, D., Matsukura, F., Omiya, T., Abe, E., Dietl, T., Ohno, Y. & Ohtani, K. Electric-field control of ferromagnetism. *Nature* **408**, 944–946 (2000).
10 Thiele, C., Dörr, K., Bilani, O., Rödel, J. & Schultz, L. Influence of strain on the magnetization and magnetoelectric effect in $La_{0.7}A_{0.3}MnO_3$/PMN-PT(001) (A = Sr, Ca). *Phys. Rev. B* **75**, 054408 (2007).
11 Vaz, C. A. F., Segal, Y., Hoffman, J., Grober, R. D., Walker, F. J. & Ahn, C. H. Temperature dependence of the magnetoelectric effect in $Pb(Zr_{0.2}Ti_{0.8})O_3$/$La_{0.8}Sr_{0.2}MnO_3$ multiferroic heterostructures. *Appl. Phys. Lett.* **97**, 042506 (2010).
12 Cherifi, R. O., Ivanovskaya, V., Phillips, L. C., Zobelli, A., Infante, I. C., Jacquet, E., Garcia, V., Fusil, S., Briddon, P. R., Guiblin, N., Mougin, A., Ünal, A. A., Kronast, F., Valencia, S., Dkhil, B., Barthélémy, A. & Bibes, M. Electric-field control of magnetic order above room temperature. *Nat. Mater.* **13**, 345–351 (2014).
13 Garcia, V., Bibes, M., Bocher, L., Valencia, S., Kronast, F., Crassous, A., Moya, X., Enouz-Vedrenne, S., Gloter, A., Imhoff, D., Deranlot, C., Mathur, N. D., Fusil, S., Bouzehouane, K. & Barthélémy, A. Ferroelectric control of spin polarization. *Science* **327**, 1106–1110 (2010).
14 Pantel, D., Goetze, S., Hesse, D. & Alexe, M. Reversible electrical switching of spin polarization in multiferroic tunnel junctions. *Nat. Mater.* **11**, 289–293 (2012).
15 Maruyama, T., Shiota, Y., Nozaki, T., Ohta, K., Toda, N., Mizuguchi, M., Tulapurkar, A. A., Shinjo, T., Shiraishi, M., Mizukami, S., Ando, Y. & Suzuki, Y. Large voltage-induced magnetic anisotropy change in a few atomic layers of iron. *Nat. Nanotechnol.* **4**, 158–161 (2009).
16 Shiota, Y., Maruyama, T., Nozaki, T., Shinjo, T., Shiraishi, M. & Suzuki, Y. Voltage-assisted magnetization switching in ultrathin $Fe_{80}Co_{20}$ alloy layers. *Appl. Phys. Express* **2**, 063001 (2009).
17 Yamada, K., Kakizakai, H., Shimamura, K., Kawaguchi, M., Fukami, S., Ishiwata, N., Chiba, D. & Ono, T. Electric field modulation of magnetic anisotropy in MgO/Co/Pt structure. *Appl. Phys. Express* **6**, 073004 (2013).
18 Kikuchi, Y., Seki, T., Kohda, M., Nitta, J. & Takanashi, K. Voltage-induced coercivity change in FePt/MgO stacks with different FePt thicknesses. *J. Phys. D: Appl. Phys.* **46**, 285002 (2013).
19 Kanai, S., Yamanouchi, M., Ikeda, S., Nakatani, Y., Matsukura, F. & Ohno, H. Electric field-induced magnetization reversal in a perpendicular-anisotropy CoFeB-MgO magnetic tunnel junction. *Appl. Phys. Lett.* **101**, 122403 (2012).
20 Shiota, Y., Nozaki, T., Bonell, F., Murakami, S., Shinjo, T. & Suzuki, Y. Induction of coherent magnetisation switching in a few atomic layers of FeCo using voltage pulses. *Nat. Mater.* **11**, 39–43 (2012).
21 Lee, J.-W., Shin, S.-C. & Kim, S.-K. Spin engineering of CoPd alloy films via the inverse piezoelectric effect. *Appl. Phys. Lett.* **82**, 2458–2460 (2003).
22 Eerenstein, W., Wiora, M., Prieto, J. L., Scott, J. F. & Mathur, N. D. Giant sharp and persistent converse magnetoelectric effects in multiferroic epitaxial heterostructures. *Nat. Mater.* **6**, 348–358 (2007).
23 Sahoo, S., Polisetty, S., Duan, C.-G., Jaswal, S. S., Tsymbal, E. Y. & Binek, C. Ferroelectric control of magnetism in $BaTiO_3$/Fe heterostructures via interface strain coupling. *Phys. Rev. B* **76**, 092108 (2007).
24 Lahtinen, T. H. E., Tuomi, J. O. & van Dijken, S. Pattern transfer and electric-field induced magnetic domain formation in multiferroic heterostructures. *Adv. Mater.* **23**, 3187–3191 (2011).
25 Venkataiah, G., Shirahata, Y., Itoh, M. & Taniyama, T. Manipulation of magnetic coercivity of Fe film in Fe/$BaTiO_3$ heterostructure by electric field. *Appl. Phys. Lett.* **99**, 102506 (2011).
26 Brivio, S., Petti, D., Bertacco, R. & Cezar, J. C. Electric field control of magnetic anisotropies and magnetic coercivity in Fe/$BaTiO_3$(001) heterostructures. *Appl. Phys. Lett.* **98**, 092505 (2011).
27 Lei, N., Park, S., Lecoeur, P., Ravelosona, D., Chappert, C., Stelmakhovych, O. & Holy, V. Magnetization reversal assisted by the inverse piezoelectric effect in Co-Fe-B/ferroelectric multilayers. *Phys. Rev. B* **84**, 012404 (2011).
28 Hsu, C. -J., Hockel, J. L. & Carman, G. P. Magnetoelectric manipulation of domain wall configuration in thin film Ni/[$Pb(Mn_{1/3}Nb_{2/3})O3$]0.68-[$PbTiO_3$]0.32(001) heterostructure. *Appl. Phys. Lett.* **100**, 092902 (2012).
29 Tsai, W.-C., Liao, S.-C., Huang, K.-F., Wang, D.-S. & Lai, C.-H. Nonvolatile electric-field modulation of magnetic anisotropy in perpendicularly magnetized $L1_0$-FePt/(001)[$Pb(Mg_{1/3}Nb_{2/3})]_{0.7}$-$(PbTiO_3)_{0.3}$ heterostructures. *Appl. Phys. Lett.* **103**, 252405 (2013).
30 Ghidini, M., Pellicelli, R., Prieto, J. L., Moya, X., Soussi, J., Briscoe, J., Dunn, S. & Mathur, N. D. Non-volatile electrically driven repeatable magnetisation reversal with no applied magnetic field. *Nat. Commun.* **4**, 1453 (2012).
31 Geprägs, S., Mannix, D., Opel, M., Goennenwein, S. T. B. & Gross, R. Converse magnetoelectric effects in Fe_3O_4/$BaTiO_3$ multiferroic hybrids. *Phys. Rev. B* **88**, 054412 (2013).
32 Bauer, U., Yao, L., Tan, A. J., Agrawal, P., Emori, S., Tuller, H. L., van Dijken, S. & Beach, G. S. D. Magneto-ionic control of interfacial magnetism. *Nat. Mater.* **14**, 174–181 (2015).
33 Borisov, P., Hochstrat, A., Chen, X., Kleemann, W. & Binek, C. Magnetoelectric switching of exchange bias. *Phys. Rev. Lett.* **94**, 117203 (2005).
34 He, X., Wang, Y., Wu, N., Caruso, A. N., Vescovo, E., Belashchenko, K. D., Dowben, P. A. & Binek, C. Robust isothermal electric control of exchange bias at room temperature. *Nat. Mater.* **9**, 579–585 (2010).
35 Wu, S. M., Cybart, S. A., Yu, P., Rossell, M. D., Zhang, J. X., Ramesh, R. & Dynes, R. C. Reversible electric control of exchange bias in a multiferroic field-effect device. *Nat. Mater.* **9**, 756–761 (2010).
36 Liu, M., Lou, J., Li, S. & Sun, N. X. E-field control of exchange bias and deterministic magnetization switching in AFM/FM/FE multiferroic heterostructures. *Adv. Func. Mater.* **21**, 2593–2598 (2011).
37 Wu, S. M., Cybert, S. A., Yi, D., Parker, J. M., Ramesh, R. & Dynes, R. C. Full electric control of exchange bias. *Phys. Rev. Lett.* **110**, 067202 (2013).
38 Pertsev, N. A. Giant magnetoelectric effect via strain-induced spin reorientation transitions in ferromagnetic films. *Phys. Rev. B* **78**, 212102 (2008).
39 Shirahata, Y., Wada, E., Itoh, M. & Taniyama, T. Perpendicularly magnetized spin filtering Cu/Ni multilayers. *Appl. Phys. Lett.* **104**, 032404 (2014).
40 Ruotolo, A., Bell, C., Leung, C. W. & Blamire, M. G. Perpendicular magnetic anisotropy and structural properties of NiCu/Cu multilayers. *J. Appl. Phys.* **96**, 512–518 (2004).
41 Johnson, M. T., Bloemen, P. J. H., den Broeder, F. J. A. & de Vries, J. J. Magnetic anisotropy in metallic multilayers. *Rep. Prog. Phys* **59**, 1409–1458 (1996).
42 Pertsev, N. A. & Kohlstedt, H. Magnetoresistive memory with ultralow critical current for magnetization switching. *Adv. Funct. Mater.* **22**, 4696–4703 (2012).
43 Farle, M., Mirwald-Schulz, B., Anisimov, A. N., Platow, W. & Baberschke, K. Higher-order magnetic anisotropies and the nature of the spin-reorientation transition in face-centered-tetragonal Ni(001)/Cu(001). *Phys. Rev. B* **55**, 3708–3715 (1997).
44 Kittel, C. Physical theory of ferromagnetic domains. *Rev. Mod. Phys.* **21**, 541–583 (1949).
45 Vollmer, R., Gutjahr-Löser, Th., Kirschner, J., van Dijken, S. & Poelsema, B. Spin reorientation transition in Ni films on Cu(001): the influence of H_2 adsorption. *Phys. Rev. B* **60**, 6277–6280 (1999).
46 Stearns, M. B. in *Landolt-Börnstein, New Series, Group III* (ed. Wijn H. P. J) Vol. 19a, (Springer-Verlag, Berlin, 1986).
47 Hirth, J. P. & Lothe, J. *Theory of Dislocations*, (McGraw-Hill, New York, 1968).
48 Bird, K. D. & Schlesinger, M. Giant magnetoresistance in electrodeposited Ni/Cu and Co/Cu multilayers. *J. Electrochem. Soc.* **142**, L65–L66 (1995).